Viscoelastic orthorhombic full wavefield inversion: development of multiparameter inversion methods

Gillian Royle, ExxonMobil Upstream Research Company*

SUMMARY

Full wavefield inversion (FWI) requires careful and accurate forward modeling in order to yield meaningful results. To obtain high fidelity wave propagation solutions, viscoelastic and anisotropic wave equations must be employed in order to account for dissipative and fractured media. An accurate and efficient time-domain method for viscoelastic wavefield simulation and inversion in orthorhombic media has been developed. The inversion engine computes gradients for both the velocity models as well as the attenuation (Q) models. The objective of this study is to present frameworks for multi-parameter FWI, isolate key pitfalls related to parameter sensitivity and computational cost, and propose potential solutions.

INTRODUCTION

A challenging aspect of viscoelastic FWI is accurately modeling the wave equation. Linear viscoelasticity provides a general framework to describe the anelastic wave propagation. The wave equation is typically based on a rheological model which accounts for anelasticity. This rheology must have the capacity to model linear viscoelasticity, in other words, a near-constant Q as a function of frequency. The General Maxwell Body (GMB) rheology, presented in Emmerich and Korn (1987) and further explained in Moczo and Kristek (2005), and the General Zener Body (GZB), outlined in Carcione (1993), are most commonly used. Time-domain finite-difference implementations have been developed for the GZB rheology uniquely. The GMB model, however, was found to produce more accurate Q-values. Based on verification testing with semi-analytic solutions, the GMB rheology is used to initally parameterize Q-models. GMB parameters are then translated to GZB parameters for the finite-difference formulae based on the equivalency relations outlined in Moczo and Kristek (2005). Figure 1 shows Q as a function of frequency, calculated using the GMB method, for a Q-value equal to 50.

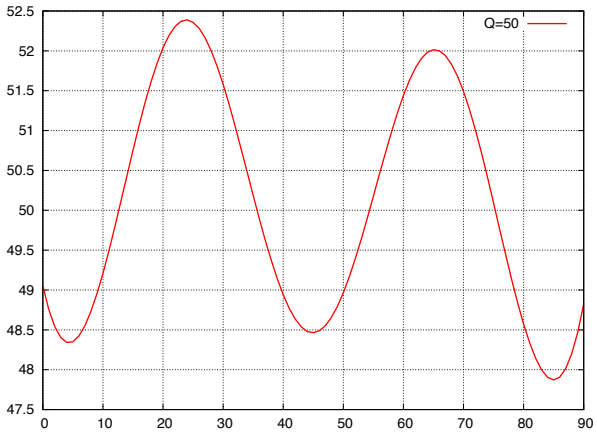

Figure 1: Q plotted as a function of frequency (Hz) using the GMB method.

Forward Modelling:

In n-dimensional media the equation of momentum conservation is

$$\rho \ddot{u}_i = \frac{\partial \sigma_{ij}}{\partial x_j} + f_i \qquad (1)$$

where u_i are the displacement field components, σ_{ij} are the stress tensor components and f_i are the body force components. For linear viscoelastic media, the relation between the components of the stress tensor σ_{ij} and strain tensor $\varepsilon_{k\ell}$ is given by the Boltzmann's superposition principle (Christensen (1982)):

$$\sigma_{ij} = \psi_{ijk\ell} * \dot{\varepsilon}_{k\ell}, \qquad k,\ell = 1,\ldots,n \qquad (2)$$

where $\psi_{ijk\ell}$ is a fourth-rank tensorial relaxation function. The asterisk denotes time convolution, and repeated indices imply summation. The wave motion is found by substitution

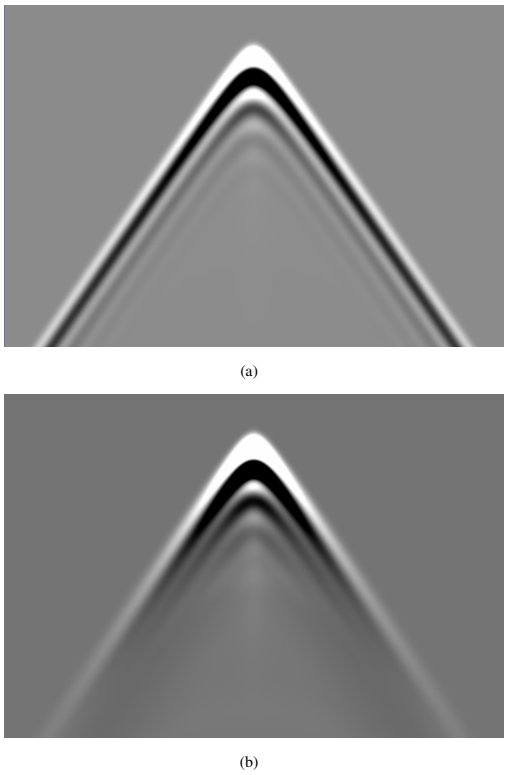

(a)

(b)

Figure 2: Vertical component synthetic seismograms using the (a) elastic wave-equation, (b) viscoelastic wave equation with $Q = 20$.

of equation (2) into equation (1). Using ψ_{ij} to denote the relaxation functions in two-index Voigt notation, and replacing the strains with spatial derivatices of displacement where $\varepsilon_{ij} = \frac{1}{2}(\frac{\partial u_i}{\partial x_j} + \frac{\partial u_j}{\partial x_i})$, the stress-strain relations for viscoelastic orthorhombic media can be written:

$$\begin{aligned}
\sigma_{xx} &= \dot{\psi}_{11} * \frac{\partial u_x}{\partial x} + \dot{\psi}_{12} * \frac{\partial u_y}{\partial y} + \dot{\psi}_{13} * \frac{\partial u_z}{\partial z} \\
\sigma_{yy} &= \dot{\psi}_{12} * \frac{\partial u_x}{\partial x} + \dot{\psi}_{22} * \frac{\partial u_y}{\partial y} + \dot{\psi}_{23} * \frac{\partial u_z}{\partial z} \\
\sigma_{zz} &= \dot{\psi}_{13} * \frac{\partial u_x}{\partial x} + \dot{\psi}_{32} * \frac{\partial u_y}{\partial y} + \dot{\psi}_{33} * \frac{\partial u_z}{\partial z} \\
\sigma_{yz} &= \dot{\psi}_{44} * (\frac{\partial u_y}{\partial z} + \frac{\partial u_z}{\partial y}) \\
\sigma_{xz} &= \dot{\psi}_{55} * (\frac{\partial u_x}{\partial z} + \frac{\partial u_z}{\partial x}) \\
\sigma_{xy} &= \dot{\psi}_{66} * (\frac{\partial u_x}{\partial y} + \frac{\partial u_y}{\partial x})
\end{aligned} \tag{3}$$

The Boltzmann's superposition principle is not easily implemented in time-domain wavefield simulations due to the convolutional kernels in equation (2). Carcione et al. (1988b,a), Robertsson et al. (1994), Charara (1996) and Hestholm (1999) all indicate how to implement a series of memory variables in place of the relaxation mechanisms in order to be rid of the convolutional kernels. Figure 2 shows two vertical-component synthetic seismograms. The first corresponds to propagation in elastic media, the second corresponds to viscoelastic propagation with $Q = 20$.

Inversion:
The inversion methodology was developed from the works of Charara (1996) and Royle (2010). In the inversion framework, the Q-models are parameterized by the relaxation functions whereas the velocity models are parameterized by the Lamé parameters. Because seismic data is significantly more sensitive to Lamé parameters than to relaxation functions, FWI is substantially more successful for velocity models than for Q-models. Gradient computations calculated using the L_2-norm are based on the magnitude of the energy in the residual wavefield. Figure 3 illustrates a simple experiment to illustrate this point. A viscoelastic wavefield is propagated through homogeneous V_p, V_s, Q_p and Q_s models. A perturbation of 1% of the initially homogeneous model is inserted, one model at a time, for each of the four models. The wavefield is repropagated. The difference between the initial wavefield and the final wavefield corresponds to the amount of residual energy in (a) the horizontal components velocity which is read by the horizontal component seismometer (a) and vertical component velocity, read by the vertical component seismometer. This indicates that the gradient calculations preferentially update velocity models, and that Q-model updates are poorly defined in comparison.

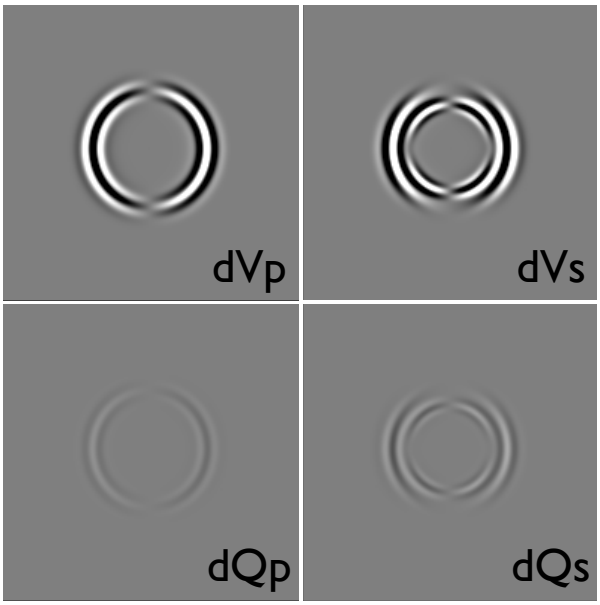

(a)

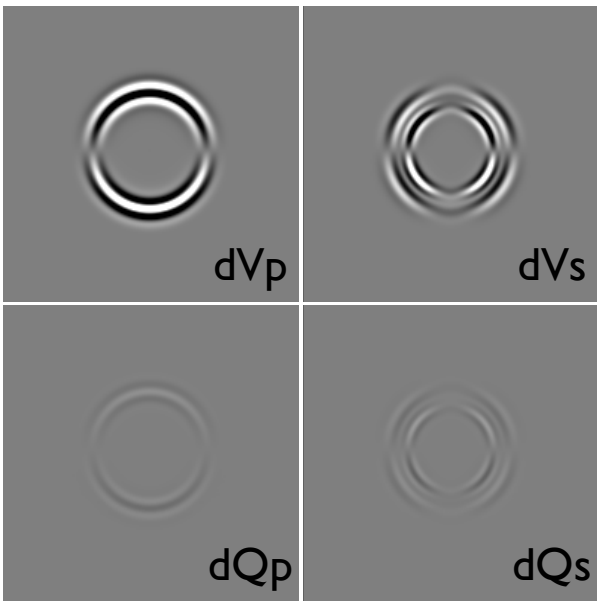

(b)

Figure 3: (a) Horizontal-component velocity field resulting from perturbations of 1% of the model. (b) Vertical-component velocity field resulting from perturbations of 1% of the model.

DISCUSSION

A series of synthetic 3D experiments will illustrate how the *completeness* of the physics in the wave equation impacts the

accuracy of the wavefield, and in particular, alters the results from FWI. Experiments will compare scenarios for acoustic, elastic, and viscoelastic wavefields in both isotropic and orthorhombic media. Comparisons of results will be based on the completeness of the wave-equation, accuracy of the wavefield simulation, accuracy of the FWI result, and computational expense. Complications that arise from multi-parameter inversion will be presented and potential remedies proposed. Experiments will include 3D problems that are designed to contain properties of realistic reservoir environments.

ACKNOWLEDGMENTS

The author would like to acknowledge Stig Hestholm and John Anderson for help and guidance in developing the viscoelastic orthorhombic simulator, Huseyin Denli for useful dicussion on rheological models for Q-modelling, and the management of ExxonMobil Upstream Research Company for permission to present this work.

REFERENCES

Carcione, J., 1993, Seismic modeling in viscoelastic media: Geophysics, **58**, 110–120.

Carcione, J., D. Kosloff, and R. Kosloff, 1988a, Viscoacoustic wve propagation simulation in the earth: Geophysics, **53**, 769–777.

———, 1988b, Wave propagation simulation in a linear viscoacoustic medium: Geophys. J. Roy. Astr. Soc., **93**, 393–407.

Charara, M., 1996, Tomographie d'un milieu visco-élastique par ajustement de la forme d'onde: PhD thesis, Institut de Physique du Globe de Paris.

Christensen, R., 1982, Theory of viscoelasticity: An introduction: Academic Press.

Emmerich, H., and M. Korn, 1987, Incorporation of attenuation into time-domain computations of seismic wave fields: Geophysics, **52**, 1252–1264.

Hestholm, S., 1999, Three dimensional finite difference viscoelastic wave modeling including surface topography: Geophysical Journal International, **139**, 852–878.

Moczo, P., and J. Kristek, 2005, On the rheological models used for time-domain methods of seismic wave propagation: Geophys. Res. Lett., **32**, L01306.

Robertsson, J., J. Blanch, and W. Symes, 1994, Viscoelastic finite-difference modeling: Geophysics, **59**, 1444–1456.

Royle, G., 2010, Viscoelastic full waveform inversion for ocean-bottom cable seismic data: PhD thesis, Institut de Physique du Globe de Paris.